PROTEINS
STRUCTURE ■ FUNCTION ■ BIOINFORMATICS

Unprecedented access of phenolic substrates to the heme active site of a catalase: Substrate binding and peroxidase-like reactivity of *Bacillus pumilus* catalase monitored by X-ray crystallography and EPR spectroscopy

Peter C. Loewen,[1]* Jacylyn Villanueva,[1] Jacek Switala,[1] Lynda J. Donald,[1] and Anabella Ivancich[2]*

[1] Department of Microbiology, University of Manitoba, Winnipeg, Manitoba R3T 2N2, Canada

[2] CNRS, Unité de Recherche Mixte CNRS/Aix-Marseille Université (UMR 7281), Laboratoire de Bioénergétique et Ingénierie des Protéines, Marseille, France.

ABSTRACT

Heme-containing catalases and catalase-peroxidases catalyze the dismutation of hydrogen peroxide as their predominant catalytic activity, but in addition, individual enzymes support low levels of peroxidase and oxidase activities, produce superoxide, and activate isoniazid as an antitubercular drug. The recent report of a heme enzyme with catalase, peroxidase and penicillin oxidase activities in *Bacillus pumilus* and its categorization as an unusual catalase-peroxidase led us to investigate the enzyme for comparison with other catalase-peroxidases, catalases, and peroxidases. Characterization revealed a typical homotetrameric catalase with one pentacoordinated heme b per subunit (Tyr340 being the axial ligand), albeit in two orientations, and a very fast catalatic turnover rate ($k_{cat} = 339{,}000\ s^{-1}$). In addition, the enzyme supported a much slower ($k_{cat} = 20\ s^{-1}$) peroxidatic activity utilizing substrates as diverse as ABTS and polyphenols, but no oxidase activity. Two binding sites, one in the main access channel and the other on the protein surface, accommodating pyrogallol, catechol, resorcinol, guaiacol, hydroquinone, and 2-chlorophenol were identified in crystal structures at 1.65–1.95 Å. A third site, in the heme distal side, accommodating only pyrogallol and catechol, interacting with the heme iron and the catalytic His and Arg residues, was also identified. This site was confirmed in solution by EPR spectroscopy characterization, which also showed that the phenolic oxygen was not directly coordinated to the heme iron (no low-spin conversion of the Fe^{III} high-spin EPR signal upon substrate binding). This is the first demonstration of phenolic substrates directly accessing the heme distal side of a catalase.

Proteins 2015; 83:853–866.

Key words: peroxidase; heme; compound I; ferryl intermediate; KatG.

INTRODUCTION

Proteins with catalase activity appeared early in evolution and have proliferated throughout most aerobic organisms as a means of protecting cells against damage from the breakdown products of H_2O_2, specifically the very reactive hydroxyl radical. Catalases are phylogenetically grouped into three families, the heme-containing catalases, the heme-containing catalase-peroxidases (KatGs) and the manganese-containing catalases. Most aerobic organisms express one or more, but there is significant variation in both the number and type of catalase with no apparent pattern across species.

Grant sponsor: Natural Sciences and Engineering Research Council (NSERC) of Canada; Grant sponsor: Canada Research Chair Program; Grant sponsor: French CNRS/UMR 8221; Grant sponsor: CEA-Saclay; Grant sponsor: CNRS Program PICS-Canada (Grant number 05865); Grant sponsor: National Research Council Canada; Grant sponsor: Canadian Institutes of Health Research; Grant sponsor: Province of Saskatchewan; Grant sponsor: Western Economic Diversification Canada; Grant sponsor: University of Saskatchewan.
*Correspondence to: Peter C. Loewen, Department of Microbiology, University of Manitoba, Winnipeg, MB R3T 2N2, Canada. E-mail: Peter.Loewen@umanitoba.ca (or) Anabella Ivancich, CNRS, Unité de Recherche Mixte CNRS/Aix-Marseille Université (UMR 7281), Laboratoire de Bioénergétique et Ingénierie des Protéines. 31 Chemin Joseph Aiguier, 13009 Marseille, France.
E-mail: aivancich@imm.cnrs.fr
Received 30 October 2014; Revised 19 January 2015; Accepted 28 January 2015
Published online 7 February 2015 in Wiley Online Library (wileyonlinelibrary.com). DOI: 10.1002/prot.24777

For example, among bacteria most *Mycobacterium* species express only one catalase-peroxidase whereas *Escherichia coli* encodes one heme catalase and one catalase-peroxidase and *Bacillus subtilis* encodes three heme catalases. Similarly, among eukaryotes, the number of heme catalases can vary from one in mammals to four in plants with some fungi expressing an additional catalase-peroxidase.[1]

The catalase reaction or dismutation of two molecules of H_2O_2 to water and molecular oxygen ($2H_2O_2 \rightarrow 2H_2O + O_2$) occurs in two steps with H_2O_2 serving as both an oxidant and a reductant. In the first step of the reaction in heme catalases, one H_2O_2 oxidizes the heme to a ferryl-oxo porphyryn radical intermediate commonly called Compound I ($H_2O_2 + Fe^{III}$ Por $\rightarrow H_2O + Fe^{IV}$=O Por$^{\bullet+}$). In the second step, H_2O_2 reduces Compound I back to the resting state ($H_2O_2 + Fe^{IV}$=O Por$^{\bullet+} \rightarrow H_2O + O_2 + Fe^{III}$ Por). The peroxidase reaction differs with Compound I being reduced back to the resting state in two steps via Compund II (Fe^{IV}-OH Por) using organic electron donors.

A recent report described the characterization of a protein with catalase and peroxidase activities from the soil bacterium *Bacillus pumilus*, and categorized it as a member of the bifunctional catalase-peroxidase (KatG) family, despite a number of unusual properties that set it apart from typical KatGs.[2] These included a β-lactam oxidase activity, a much smaller subunit size and no apparent sequence similarity to KatGs. The putative expression of a single catalase-peroxidase in a soil bacterium was also unusual in comparison with other *Bacillus* species, which usually encode one or more heme catalases.[3] While both bovine liver catalase (BLC)[4] and the large subunit *Scytalidium thermophilum* catalase[5–8] have been reported to support oxidase activities, the only previously reported oxidase activity of catalase-peroxidases was that of a low level NADH oxidase for *Burkholderia pseudomallei* KatG.[9] Furthermore, there has been one report of a polyphenol peroxidase activity associated with BLC.[10]

In this report, we have undertaken a comprehensive structural and kinetic investigation of this intriguing heme enzyme with associated catalase, peroxidase, and oxidase activities. Our recently reported genomic sequence has revealed that the *B. pumilus* (BPC) strain does not encode a catalase-peroxidase, but does harbor two heme catalase genes, one of which lacks an initiation codon and appears to be cryptic or not expressed.[11] Accordingly, biochemical and X-ray crystallography analyses revealed that the expressed catalase exhibited properties consistent with those of other well-characterized heme catalases, but with one very significant difference. That is that the enzyme exhibited a significant peroxidase activity, and binding sites for a number of polyphenol substrates (commonly used as substrates in peroxidases) were identified by X-ray crystallography. The binding site in close proximity to the heme was also characterized by monitoring the modifications on the ferric EPR spectrum resulting from changes in the heme microenvironment upon incubation with the different substrates. An oxidase activity was not detected. Based on this unprecedented observation of phenolic substrate binding in the heme cavity and access channel of a catalase, the structural determinants of the peroxidase reaction of catalases have been better defined and are in some ways comparable to those of KatGs.

MATERIALS AND METHODS

Chemicals and media

All chemicals were obtained from Sigma-Aldrich or Fisher unless otherwise stated. All media components were obtained from Becton-Dickson and all restriction enzymes were obtained from Invitrogen.

Protein purification and characterization

The catalase protein was first isolated directly from BPC MTCC B6033 grown for 16 h at 37 °C in a medium containing 0.5% peptone, 0.2% beef extract, 0.1% yeast extract, and 0.5% NaCl. Crude extracts were prepared and the protein purified as previously described for *E. coli* KatE (excluding the Bio-Gel fractionation step).[12] The purified protein was kinetically characterized following the protocols previously employed making it possible to accurately compare these data with those of 16 other catalases.[13]

Enzyme assays

Catalase activity was determined by the method of Rørth and Jensen[14] in a Gilson oxygraph equipped with Clark electrode. One unit of catalase is defined as the amount that decomposes 1 μmole of H_2O_2 in 1 min in a 60 m*M* H_2O_2 solution at pH 7.0 and 37 °C. Peroxidase activity was determined in two ways. In the first, using ABTS [2,2′-azinobis(3-ethylbenzothiazolinesulfonic acid)] (ε_{405}= 36,800 M^{-1} cm^{-1}),[15] one unit is defined as the amount that decomposes 1 μmol ABTS in a solution of 0.4 m*M* ABTS and 0.5 m*M* peroxyacetic acid at pH 4.5 and 25 °C. In the second, the rate of reduction of BPC catalase Compound I was used,[16] because the autocatalytic oxidation rate of the polyphenols was sufficiently high that the direct spectrophotometric measurement of their oxidation by BPC catalase was not possible. A solution of 1.25 μ*M* enzyme in 50 m*M* potassium phosphate pH 6.5 was mixed with 12.5 μ*M* of peroxyacetic acid, also in 50 m*M* potassium phosphate buffer at pH 6.5, and let sit for 1 min to generate Compound I, as monitored by the characteristic electronic-absorption spectral changes (decrease in intensity and maximum shift from 406 to 411 nm of the heme Soret band).

Then polyphenols from 0.1 to 1.0 m*M* were added and the increase in absorbance at 411 nm was measured for a period of 5 min. The polyphenols studied included pyrogallol (1,2,3-trihydroxybenzene), catechol (1,2-dihydroxybenzene), resorcinol (1,3-dihydroxybenzene) hydroquinone (1,4-dihydroxybenzene), guaiacol (1-hydroxy-2-methoxybenzene), and 2-chlorophenol.

Cloning of katX1 and katX2 and expression of recombinant KatX2

Based on the genomic sequence of BPC B6033 (CP007436.1),[11] two sets of primers bracketing *katX1* and *katX2* were constructed (for *katX1*, 5′-GTCAGAAG AAAGCTTGACGAATCG and 5′-GTGAGGCGACCTAGG AAAAAAGTA; for *katX2*, 5-′GATTGCTAGAAAGCTTTT TTGTTTAC and 5′-AAAAAGAGGGGATCCAGCTGAAA AG) and used to PCR amplify the *katX1* cryptic gene and the *katX2* gene for cloning into pBluscript vector generating pKatX1 and pKatX2. Their sequences were verified and they were transformed into UM255[17] (*katE* and *katG* deficient) for expression of KatX2 protein and its purification.[13] No protein was expressed from the pKatX1 clone regardless of the orientation in the vector. Hence, the only heme catalase expressed in BPC B6033 is KatX2, which will be referred to as BPC (for Bacilus pumilus catalase). The *katX2* gene was also cloned into pACYCduet-FC encoding ferrochelatase for coexpression.[18] The BPC protein in *E. coli* extracts exhibited migratory properties on nondenaturing gel electrophoresis identical to the purified catalase isolated directly from BPC and to the catalase activity in crude extracts of BPC.

Crystallization of the recombinant KatX2 from *Bacilus pumilus* catalase

Crystals were obtained at room temperature by the vapor diffusion hanging drop method at 20 °C using an equilibration solution containing 0.1*M* sodium acetate pH 4.6, 50 m*M* NaCl, 10 m*M* $CoCl_2$, and 12–20% 2-methyl-2,4-pentanediol and a 12 mg/mL protein solution prepared by mixing in a 2 to 1 ratio the protein in 50 m*M* pH 6.5 potassium phosphate buffer and the equilibration solution. Crystals were monoclinic, in space group $P2_1$ with four subunits in the crystal asymmetric unit. Diffraction data were collected using synchrotron beam line CMCF 08ID-1 at the Canadian Light Source in Saskatoon, SK from crystals flash cooled in reservoir buffer and cooled with a nitrogen cryostream. For enzyme-substrate complexes, crystals were soaked for 1 min in a solution of 100 m*M* substrate in mother liquor. Data were processed and scaled using XDS[19] MOSFLM[20] and SCALA,[21] respectively, as part of the CCP4 software suite[22] (Table I). The structure determination of the native enzyme was carried out with MOLREP[22] using *Helicobacter pylori* catalase[23] (PDB accession 1QWL with 54% sequence identity over the N-terminal 360 residues) as the initial searching model. Refinement of the ligand complexes started with a rigid body refinement using the native enzyme solution. Structure refinement was completed using REFMAC[24] and manual modeling with the molecular graphics program COOT.[25] The Ramachandran distribution of residues was ∼ 96.8, 2.6, and 0.5% in the favored, allowed and outlier regions, respectively. Figures were generated using PYMOL (The PYMOL Molecular Graphics System, Schrodinger, LLC). The cavities associated with the main channel were visualized with HOLLOW.[26]

Electron paramagnetic resonance (EPR) spectroscopy

The 9-GHz EPR spectra were recorded on a Bruker EleXsys E500 spectrometer equipped with a standard Bruker ER 4102 X-band resonator and a liquid helium cryostat (Oxford Instruments, ESR 900). The spectra for the ferric BPC catalase at pH 6.0 and pH 8.0, were recorded before and after incubation of the enzyme with catechol, pyrogallol, and guaicol. To avoid significant changes of pH upon freezing we used Tris-maleate buffer, which covers the range $5.20 \leq pH \leq 8.60$ with minor changes upon freezing (0.1 pH unit all through the range). Centricon microconcentrators (Amicon) were used for the buffer exchange. Typically, EPR samples of ferric BPC catalase at 0.3 m*M* (heme) concentration were measured in 4-mm quartz tubes. To achieve binding of the substrates to the heme site, 4 μL substrate at 1*M* concentration was added to 60 mL enzyme at 0.3 m*M* concentration (a 200 fold-excess of substrate, prepared in the same buffer and pH as the enzyme) and incubated for 2 h at room temperature (20 °C) followed by 12 h incubation in the fridge (8 °C). Samples of commercial catalase from bovine liver, further purified as previously described,[27] were used for comparisons of pH and substrate binding effect on the EPR ferric signal. EPR samples of BLC were prepared in identical experimental conditions as described above for the BPC catalase.

RESULTS

Genomic sequence of BPC B6033

Our initial impetus for the current work was the report that BPC B6033 expressed an unusual catalase-peroxidase[2], and the first step taken was a determination of the strain's genomic sequence (NCBI accession CP007436).[11] It proved to be similar to the previously reported genome of BPC SAFR-032[28] with >85% sequence identity, albeit with one deletion of about 40,000 bp. A survey of the genome for catalase genes revealed one heme catalase gene, labeled *katX2* (after the SAFR-032 annotation) and two manganese catalase

Table I
Data Collection and Refinement Statistics of BPC and BPC Bound with Various Polyphenol Ligands

A: Data collection statistics							
PDB	4Q0L BPC	4Q0M BPC + pyrogallol	4Q0N BPC + catechol	4Q0O BPC + resorcinol	4Q0P BPC- + hydroquinone	4Q0Q BPC + guaiacol	4Q0R BPC + chlorophenol
Unit cell parameters							
Space group	$P2_1$	$P2_1$	$P2_1$	$P2_1$	$P2_1$	$P2_1$	$P2_1$
a (Å)	91.647	91.853	92.140	91.907	92.279	91.790	91.660
b (Å)	109.191	109.424	109.116	108.597	109.455	108.109	109.080
c (Å)	102.829	103.368	103.695	103.524	104.199	103.409	103.030
β (°)	91.67	92.21	92.20	92.01	92.05	91.98	91.9
Resolution[a]	48.22–1.65 (1.74–1.65)	45.9–1.65 (1.74–1.65)	48.30–1.80 (1.90–1.80)	48.08 −1.75 (1.84–1.75)	48.44–1.90 (2.00–1.90)	47.90–1.70 (1.79–1.70)	30.53–1.95 (2.06–1.95)
Unique reflections	233,888 (33,855)	237,624 (35,613)	173,800 (26,631)	197,688 (29,519)	149,181 (22,528)	210,092 (31,667)	138,428 (19,314)
Completeness (%)	96.7 (95.9)	97.2 (99.8)	92.3 (96.8)	97.0 (99.3)	91.9 (95.3)	95.2 (98.6)	94.1 (90.2)
R_{merge}	0.068 (0.414)	0.068 (0.322)	0.069 (0.354)	0.063 (0.423)	0.092 (0.473)	0.068 (0.400)	0.095 (0.415)
$\langle I/\sigma I \rangle$	10.0 (2.5)	8.4 (2.2)	7.6 (2.1)	9.5 (2.1)	7.5 (1.9)	9.4 (2.4)	7.1 (2.0)
CC(1/2)	0.997 (0.827)	0.997 (0.937)	0.994 (0.844)	0.997 (0.858)	0.994 (0.918)	0.996 (0.806)	0.992 (0.802)
Multiplicity	2.8 (2.8)	2.9 (2.9)	2.2 (2.1)	2.5 (2.5)	2.7 (2.6)	2.7 (2.7)	2.7 (2.6)
B: Model refinement statistics							
No. reflections	222,110	225,265	164,090	187,173	140,117	199,503	131,285
R_{cryst} (%)	17.1	17.7	20.6	17.9	23.0	16.2	18.2
R_{free} (%)	19.9	21.0	23.8	20.9	26.2	19.0	22.0
Non-H atoms	16,196	16,208	16,239	16,235	16,204	16,264	16,234
Water molecules	1750	1728	1696	1608	1495	1706	1671
Average B-factor $Å^2$							
Protein	19.75	22.65	22.34	25.69	28.40	21.55	23.71
Heme	11.64	14.78	14.03	16.74	19.40	13.54	15.25
Waters	26.82	29.36	29.08	31.54	31.72	28.86	28.51
Other							
Coor. err. (Å)[b]	0.077	0.081	0.120	0.098	0.153	0.078	0.130
rms dev. bonds (Å)	0.018	0.019	0.017	0.018	0.014	0.019	0.015
rms dev. angles (°)	1.76	1.85	1.67	1.75	1.52	1.80	1.58

[a]Values in parentheses correspond to the highest resolution shell.
[b]Based on maximum likelihood.

genes. There was one additional heme catalase gene (*katX1* in the SAFR-032 annotation), but it lacked both an N-terminal methionine and a recognizable ribosome binding sequence suggesting it was a cryptic or unexpressed gene. This was confirmed by the lack of expression of any protein from the cloned *katX1* gene, whereas the *katX2* gene supported the expression of protein. Phylogenetic analysis placed the KatX2 protein in Clade 1 of the monofunctional catalases. No protein encoded by the genome was found containing the sequence RLYREHRPEEPP[2] originally associated with the unusual catalase-peroxidase.

Enzymatic reactivity

The enzyme was first purified directly from extracts of BPC B6033 yielding a protein >85% pure by SDS PAGE with a subunit size of ~58 kDa and a UV–visible electronic absorption spectrum typical for heme b-containing catalases.[27] Expression of the cloned *katX2* gene in *E. coli* and subsequent purification yielded a protein with similar subunit size with an apparent K_M for H_2O_2 of 65 m*M* and a maximal turnover rate of 339,000 s^{-1}, which is among the highest so far determined for a catalase.[13] Electrospray mass spectrometry confirmed that BPC was a tetramer as expected. In addition, the ferric EPR spectrum of the enzyme purified directly from BPC was very similar to that of the recombinant enzyme (see below).

The catalase isolated from BPC was originally reported to catalyze the oxidation of penicillin G using molecular oxygen,[2] and this reaction was investigated further. Despite many attempts, no penicillin G oxidase activity in excess of the very high background rate could be reliably measured, and no oxygen uptake was observed during a prolonged incubation in an oxygraph. BLC has also been reported to oxidize a variety of substrates using molecular oxygen as the electron acceptor.[4] We were able to confirm the oxidase reaction in BLC only using 10-acetyl-3,7-dihydroxyphenoxazine as substrate, but BPC did not catalyze that oxidation in a parallel experiment. Similarly, no oxidation of pyrogallol, catechol, or hydroquinone could be measured by BLC, BPC, or *E. coli* KatE either by measuring changes in the very high background

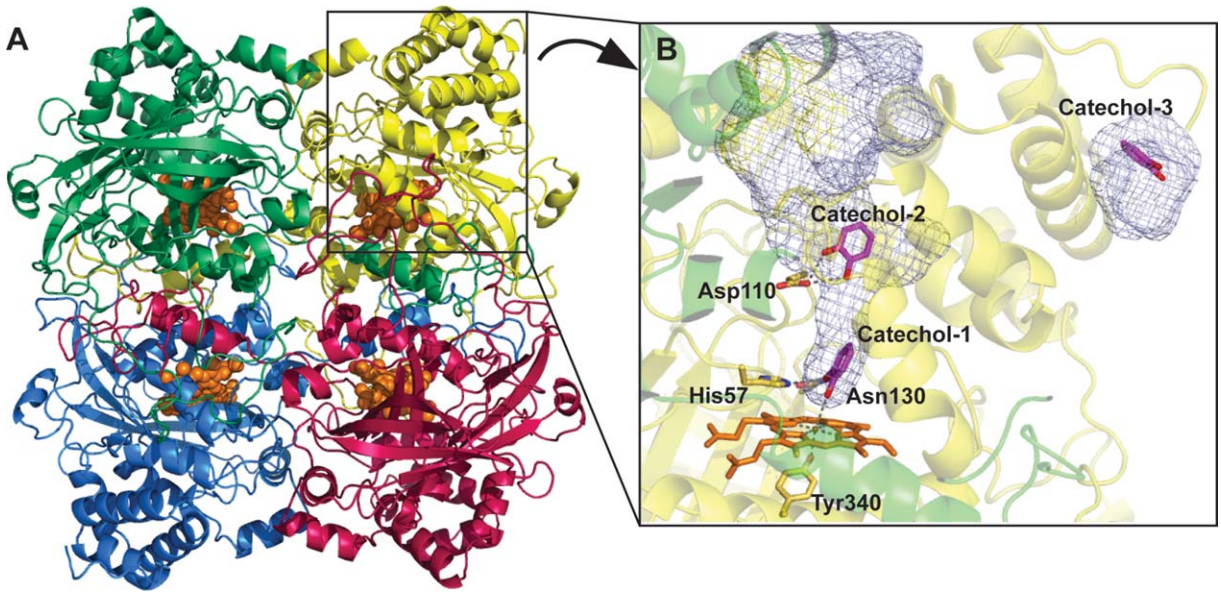

Figure 1

Structure of BPC catalase and its main channel. In panel A, the tetramer is viewed looking down the two-fold axis. The tetrameric composition is delineated by the different color for each subunit. The hemes bound to each subunit are colored orange. In panel B, the main access channel to the heme active site and a pocket on the surface are delineated by the blue mesh. The three binding sites of catechol molecules are shown.

rates of absorbance at 420 nm or by O_2 consumption. We conclude that BPC does not support an oxidase reaction.

A peroxidase-like reaction with pyrogallol as substrate has been reported for BLC,[10] and we therefore investigated BPC for a similar reactivity. No reaction was observed in a standard peroxidase assay utilizing H_2O_2 as oxidant, presumably because H_2O_2 was a much better reductant of Compound I than the peroxidatic substrates. However, with peroxyacetic acid as oxidant, a low-level peroxidase activity of 11.0 nmol ABTS $nmol^{-1}$ heme s^{-1} at pH 4.5 was observed. A direct spectrophotometric assay for the oxidation of polyphenols proved unsuccessful with no observable activity below pH 8 and high background levels of substrate oxidation above pH 8. However, it was possible to monitor the rate of Compound I ($Fe^{IV}=O$ $Por^{\bullet+}$) reduction to resting state (Fe^{III} Por),[16] which revealed rates of 13.4, 9.7, and 5.1 M^{-1} s^{-1}, respectively for guaiacol, hydroquinone, and pyrogallol. These peroxidatic rates are similar to those reported for catalase-peroxidases.[16,29] It is of note that because of the multiple binding sites for each of the substrates, identified in the crystal structures of BPC-substrate complexes (see below), the measured rates most likely reflect an average of different peroxidatic reactions, involving direct electron (and proton) transfer to the oxyferryl oxygen and long-range electron transfer to the Compound I intermediate, and/or a protein-based high-valent heme intermediate. In the case of catalase-peroxidases, substrates cannot access the heme site,[30] hence the reaction with substrate(s) proceeds via a long-range electron transfer to the heme of the Compound I intermediate in the case of *Synechocystis* KatG,[31] or through one of the [$Fe^{IV}=O$ $Trp^{\bullet}$] intermediates formed subsequently to Compound I in the KatGs from *M. tuberculosis*[32] and *B. pseudomallei*.[30,33]

Crystal structure of *Bacilus pumilus* catalase

To characterize BPC further, the protein was successfully crystallized as large dark brown-red cubic crystals that diffracted well in space group $P2_1$. Using the structure of a subunit of *H. pylori* catalase[23] as the probe, a molecular replacement solution containing four subunits was found. While the cores of the four subunits closely traced the electron density, the N-terminal 30 and C-terminal 100 residues required extensive rebuilding to fit the maps. The final structure was refined to 1.65 Å with R and R_{free} values of 17.4 and 19.8%, respectively (Table I).

The structure of BPC is that of a typical small subunit catalase with four identical subunits containing the expected highly conserved catalytic residues (His57 and Asn130) in the heme cavity and the highly (100%) conserved aspartate (Asp110) in the main channel [Fig. 1(A)]. The main channel leading to the heme cavity is funnel shaped and similar in dimensions to that of HPC, BLC, and human erythrocyte catalase (HEC [Fig. 1(B)]. There is a well-resolved matrix of high occupancy water molecules leading into the channel terminated by a single

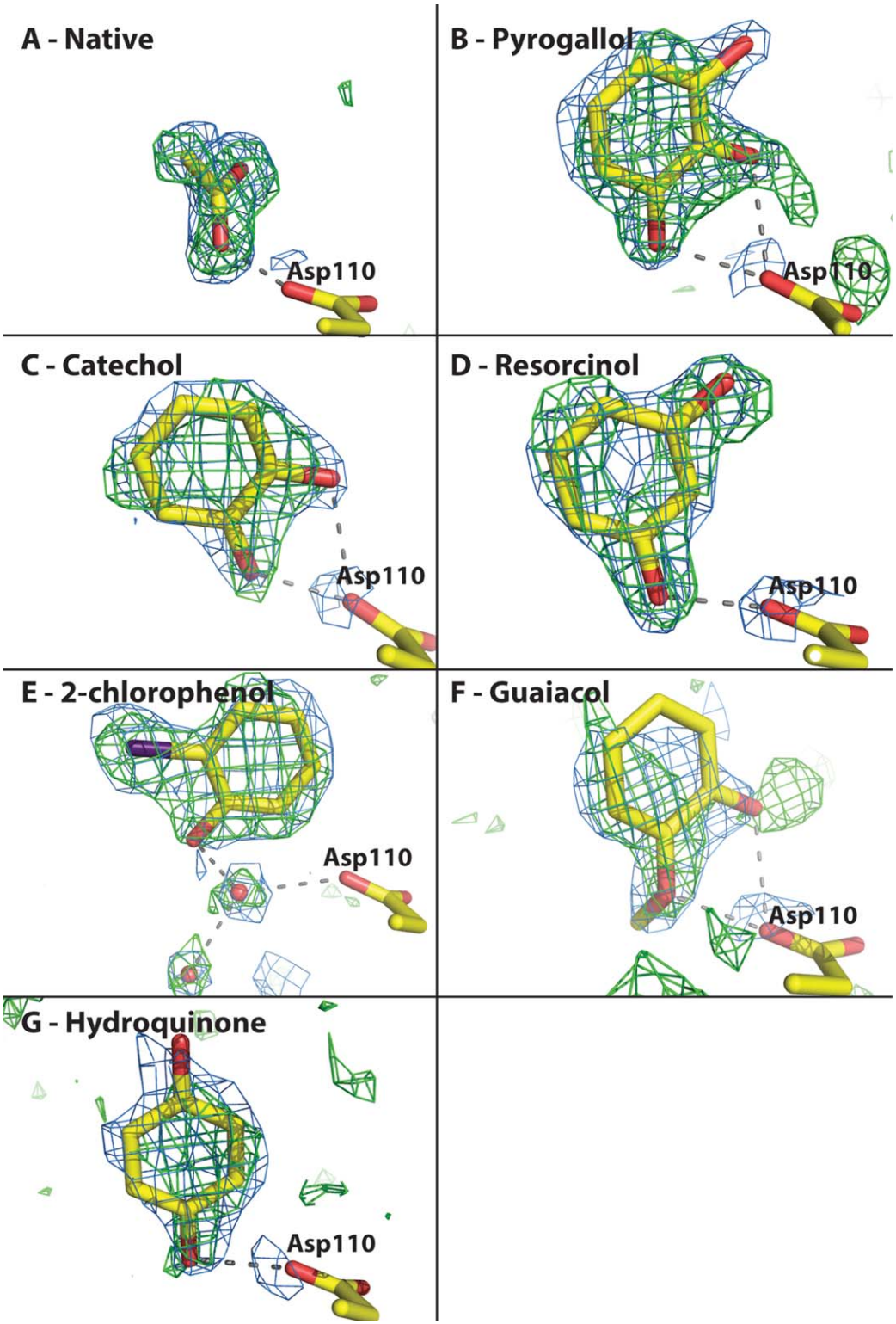

Figure 2

View of the substrate binding sites in the main channel of BPC catalase. The native structure with one acetate is shown in panel A for comparisons. The subsequent panels show pyrogallol (panel B), catechol (panel C), resorcinol (panel D), 2-chlorophenol (panel E), guaiacol (panel F), and hydroquinone (panel G). The omit $F_o - F_c$ electron density maps indicated by the green hatching at ~3 σ were calculated without the substrates or channel waters included in the model and were added to the model afterwards. The $2F_o - F_c$ electron density maps indicated by the blue hatching at ~1 σ were calculated with the ligand in the model.

Table II
Ligand B-Factors Calculated with Occupancy of 1.00

		Subunit A			Subunit B			Subunit C			Subunit D		
Ligand	PDB	1[a]	2[b]	3[c]	1	2	3	1	2	3	1	2	3
Pyrogallol	4QOM	33.8	43.6	–	32.3	40.9	–	28.6	34.2	–	33.2	37.3	–
Catechol	4QON	42.5	27.5	–	40.4	33.1	–	45.1	25.3	–	44.1	28.3	45.5
Resorcinol	4QOO	33.9	–	–	26.4	–	–	24.6	–	–	29.2	–	–
Hydroquinone	4QOP	51.3	–	–	50.6	–	–	45.1	–	–	66.9	–	–
Guaiacol	4QOQ	59.2	–	–	53.7	–	38.6	47.8	–	–	57.8	–	45.6
2-Chlorophenol	4QOR	38.2	–	–	32.7	–	51.1	32.9	–	–	36.6	–	74.8

[a]1 is the binding site in the channel adjacent of Asp110 as in Figure 2.
[b]2 is the binding site in the heme cavity adjacent to the heme iron as in Figure 3.
[c]3 is the remote binding site adjacent to Cys461 as in Figure 4.

acetate molecule associated with the carbonyl of Asp110. The acetate is in approximately the same location as the acetate present in HEC (1DGF)[34] and the formate in HPC (1QWM).[23] The 8 Å of the channel between Asp110 and the heme is lined with hydrophobic residues including Val98, Pro111, Phe136, Val147, and Leu150 and is almost devoid of water molecules. Immediately above the heme are three waters, one in association with the catalytic His57 (2.9 Å), the second hydrogen bonded to the first water (~2.1 Å) and the third (in just three subunits) associated with the first water and the heme iron (2.2 - 3.1 Å). Surprisingly, the heme is present with equal proportions of two orientations flipped relative to one another. All clade 3 enzymes so far characterized have one orientation of heme while a clade 1 enzyme (CatF of *Pseudomonas syringae*)[35] has predominantly the flipped orientation similar to that in the large subunit KatE from *E. coli*. It is perhaps relevant that changing the residues adjacent to the heme in KatE did influence the heme orientation leading to mixtures.[36] Unfortunately, it is not yet possible to draw simple rules about what determines the heme orientation, but it is possible to conclude that the heme orientation does not significantly influence the rate of catalytic turnover. As in other catalases, the residue blocking the lateral channel leading out of the heme cavity (Val199) has adopted an unusual backbone geometry that falls outside the normal Ramachandran acceptable regions. This is also the path to the NADH binding site in catalases that bind the cofactor, but in BPC, the lateral channel is very short containing only 3 or 4 well defined waters before opening to a broad cavity on the exterior of the protein where there is no evidence of NADH binding in the form of extra electron density.

Identification of polyphenol binding sites in *Bacilus pumilus* catalase

The demonstration of a peroxidase activity implied the existence of one or more binding sites for the peroxidatic substrates, and to identify such sites, crystals of BPC were soaked in mother liquor containing a variety of different phenol derivatives. Ultimately, three distinct binding sites were identified, one in the main access channel associated with Asp110 about 12 Å from the heme, a second in the heme cavity with one oxygen located 2.8 Å from the heme iron and a third on the protein surface remote from the heme [Fig. 1(B)]. The main channel site appears to accept the broadest range of polyphenols being occupied with varying occupancies by all six that were investigated, including pyrogallol, catechol, resorcinol, hydroquinone, guaiacol, and 2-chlorophenol (Fig. 2). Based on the ligand B-factors (Table II) and the electron density maps in Figure 2, pyrogallol and resorcinol bound with highest occupancy while hydroquinone and guaiacol had the lowest occupancy. The orientations varied slightly among the ligands but all formed one or two hydrogen bond interactions (2.4–2.9 Å) with the carboxylate of the conserved channel Asp110 either directly or, as in the case of 2-chlorophenol, through an intermediary water. The second hydrogen bond with Asp110 requires an ortho-OH as in pyrogallol, catechol, and guaiacol. The meta-OH in pyrogallol and resorcinol and para-OH in hydroquinone are more loosely hydrogen bonded either with water or the OH of Tyr164.

The unprecedented occupancy of the heme cavity of a catalase by a polyphenol is restricted to only two of the substrates tested, pyrogallol and catechol (Fig. 3), with the smaller catechol having slightly higher occupancy based on their respective B-factors (Table II). This is presumably because an ortho configuration of two phenolic OHs is required to create a stable interaction, while replacing the structural water molecules of the native enzyme [see Fig. 3, panels (A–C)]. One OH directly interacts with the heme iron (2.7–2.9 Å) while the second forms hydrogen bonds with the Nϵ of His57 (2.4–2.8 Å) and the Nδ of Asn130 (2.7–3.0 Å), both residues having a catalytic role.[37] It is of note that one of the binding sites for formate in *H. pylori* catalase was found in a similar configuration adjacent to the heme iron and making H-bonding contacts with the distal-side His and Arg residues.[23]

The third binding site for the phenolic substrates is located on the surface of the protein ~30 Å from the heme in a pocket created by Leu457, Cys461, Tyr464,

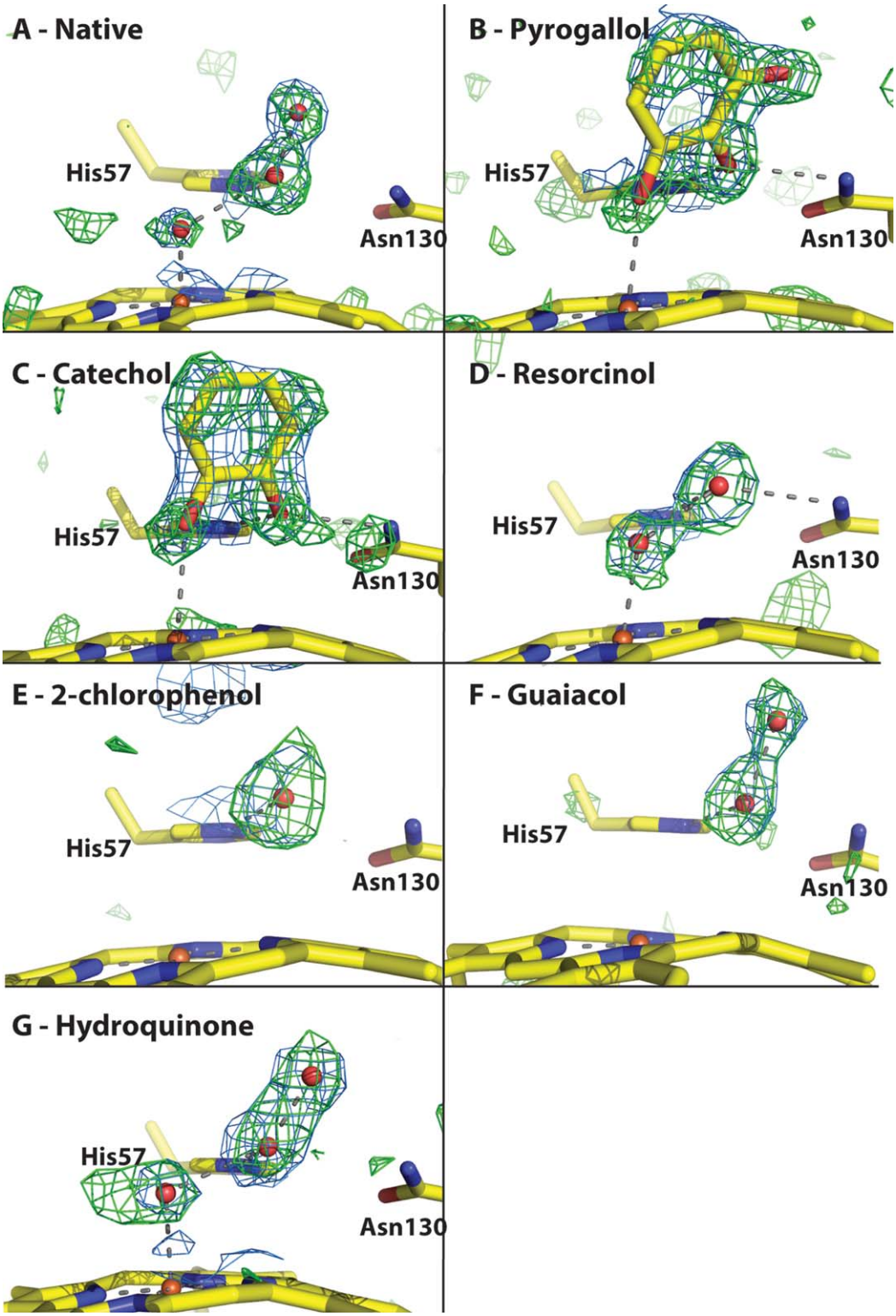

Figure 3

View of the substrates binding in the heme cavity of BPC catalase. The native structure with one acetate is shown in panel A for comparisons. The subsequent panels show pyrogallol (panel B), catechol (panel C), resorcinol (panel D), 2-chlorophenol (panel E), guaiacol (panel F), and hydroquinone (panel G). The omit $F_o - F_c$ electron density maps indicated by the green hatching at $\sim 3\ \sigma$ were calculated without the substrates or channel waters included in the model and were added to the model afterwards. The $2F_o - F_c$ electron density maps indicated by the blue hatching at $\sim 1\ \sigma$ were calculated with the ligand in the model.

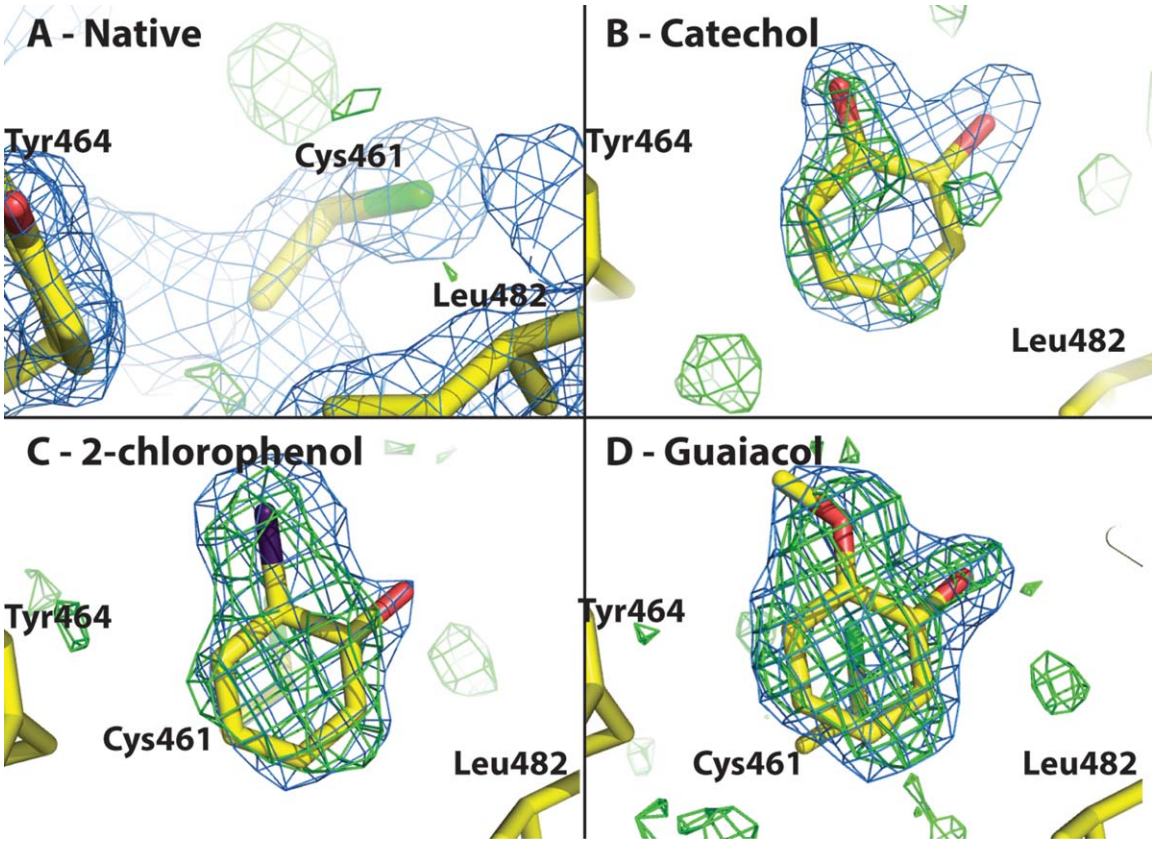

Figure 4

View of the substrates binding in the surface site of BPC catalase. The native structure in the surroundings of Cys461 with no substrate bound is shown in panel A. The subsequent panels show catechol (panel B), 2-chlorophenol (panel C), and guaiacol (panel D) bound to the enzyme. The omit F_o-F_c electron density maps indicated by the green hatching at ~3 σ were calculated without the ligand included in the model and they were added to the model afterwards. The $2F_o-F_c$ electron density maps indicated by the blue hatching at ~1 σ were calculated with the ligand in the model. 2-Chlorophenol and guaiacol exhibited the highest occupancy in two or more subunits. Catechol was present at lower occupancy and the other ligands were present at too low an occupancy to be reliably refined. Note the change in conformation of Cys461 after ligand binding in panels B, C, and D compared with the native structure in panel A. The maps in panels B, C, and D exclude the electron density corresponding to the surrounding residues, but panel A shows all the electron density in the region to illustrate the absence of anything in the region in the native structure.

Leu482, and Tyr485 (Fig. 4). This site is <15 Å from Trp165 and Tyr164 adjacent to the main channel binding site making electron transfer from the peroxidatic substrate to the oxidized heme feasible. Binding at the remote site is stabilized entirely by van der Waals contacts with the protein; no ionic or hydrogen bonds are evident. Based on the ligand B-factors (Table II) and the electron density maps, guaiacol and 2-chlorophenol exhibit highest occupancy and are present in 2 or more subunits while catechol could be refined into only one subunit. Significantly, there is a change in the conformation of Cys461 associated with substrate binding [compare the native conformer in Fig. 4(A) with the conformers in Fig. 4(D)] and this proved to be a useful indicator of partial substrate binding. For example, two conformers were evident in the electron density maps of two subunits of the BPC-resorcinol complex and in one subunit of the BPC-pyrogallol complex, along with weak and poorly defined blobs of electron density approximately where the ligand would be expected to bind. Thus, the remote site, like the main channel site, appears to accept a diversity of phenolic substrates. In the case of guaiacol binding, the protein structure was stabilized sufficiently that disorder in the terminal residues was reduced allowing one additional residue, Leu486, to be refined into the model.

Characterization of the heme active site by EPR spectroscopy: pH-dependence and binding of substrates in the heme distal-side cavity of BPC catalase

Figure 5 (top) shows the 9-GHz EPR spectra of native (resting) BPC catalase recorded at 4 K, and showing the typical pattern of a rhombically-distorted high-spin ferric heme with resonance absorption lines extending between

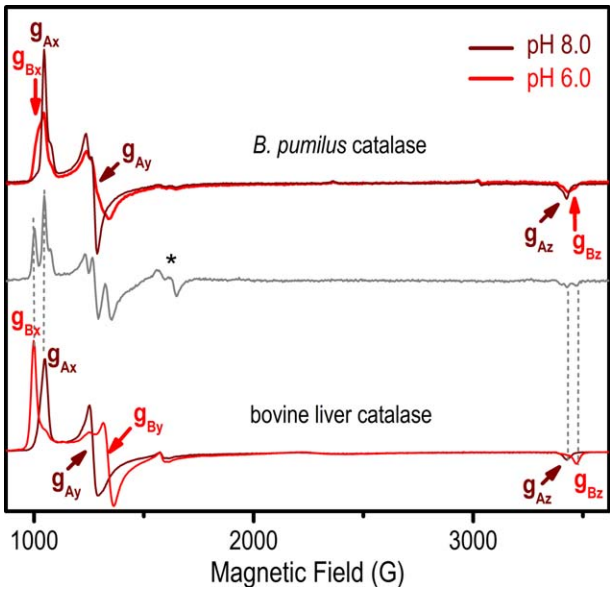

Figure 5

The 9-GHz EPR spectra of ferric BPC and BLC s at pH 6.0 (red traces) and pH 8.0 (dark red traces) values. The EPR spectrum of the nonrecombinant BPC catalase at pH 5.5 is also shown (top, gray trace) for comparisons with the *E. coli* expressed enzyme (top, red trace). Experimental conditions: spectra were recorded at 4 K, 1 mW microwave power, 4 G modulation amplitude, 100 kHz modulation frequency.

$g \approx 6$ and $g \approx 2$. At pH 8.0, the spectrum showed a predominant ferric high-spin signal (labeled g_{Ax}, g_{Ay}, g_{Az}) with effective g-values of $g_{Ax} = 6.48$, $g_{Ay} = 5.31$, and $g_{Az} = 1.98$ (Fig. 4 top, dark red trace), and the relatively lower contribution (15%) of another component with $g_x = 6.30$, $g_y = 5.31$, and $g_z = 1.99$. Not surprisingly, this spectrum is very similar to the BLC EPR spectrum at pH 8.0 (Fig. 5 bottom, dark red trace) and to those of other bacterial catalases previously reported.[27,38]

Differences in the coordination environment of the heme iron can be monitored by the extent of the rhombic distortion on the EPR spectrum, reflected by the difference between the g_x and g_y components of the g-tensor as we have shown in the case of pH-dependent EPR spectrum of *H. pylori* catalase.[23] Similarly, both BPC and BLC showed the conversion at pH 6.0 to a more rhombically distorted signal, with g^{eff}-values of $g_{Ax} = 6.78$, $g_{Ay} = 5.07$, and $g_{Az} = 1.95$ (Fig. 5 bottom, red trace) and only differing in the extent of the conversion. While BLC showed an almost complete (80%) conversion to the signal with higher rhombic distortion at pH 6.0 (Fig. 5 bottom, red trace), in BPC the conversion was 50% (Fig. 5 top, red trace). It is noteworthy that the difference between the g_x and g_y values of the two components contributing to the EPR spectrum of a rhombically distorted EPR signal are due to slightly different deviations from the tetragonal symmetry ($g_x = g_y = 6$), thus reflecting subtle, but measurable, differences in conformations of the microenvironment of the heme iron between BPC and BLC. Such a pH-induced effect was clearly observed in the case of KatGs in which there is an extended H-bonding network including structural water molecules, catalytically relevant residues on the heme distal side and the heme propionates.[39,40] The ferric EPR spectrum of non-recombinant BPC (thus directly purified from BPC extracts) at pH 6.8 (Fig. 5 top, gray trace) showed the contribution of the same signals as the enzyme expressed in *E. coli*. Also, the EPR signal at $g = 4.3$ (shown by an asterisk in Fig. 5, top, gray trace) in the nonrecombinant enzyme is indicative of a nonheme high-spin ($S = 5/2$) ferric iron in a rhombically distorted coordination environment, possibly arising from nonheme iron binding to the enzyme.

The binding of substrates in solution on the heme distal side and in close proximity to the heme iron of BPC was also characterized by monitoring the modifications on the ferric EPR spectrum upon incubation of the enzyme with the different substrates. Only the BPC samples incubated in catechol and in pyrogallol showed clear changes on their ferric high-spin EPR spectrum, as shown in Figure 6. The absence of a low-spin ferric signal in the EPR spectrum of BPC before or after incubation with the substrates unequivocally shows that, despite the proximity of the phenolic oxygen(s) of catechol and pyrogallol (see previous section) they do not coordinate to the heme iron. This is a similar situation to that observed in the case of the formic acid bound to *H. pylori* catalase,[23] both in the crystal structure and through the spectral changes induced in the ferric high-spin EPR spectrum. In particular, the ferric EPR spectrum of BPC at pH 6.5 [Fig. 6(A), black trace] showed clear changes upon incubation with catechol [Fig. 6(B), red trace] and pyrogallol [Fig. 6(B), green trace], the disappearance of the component with g^{eff}-values of $g_{Ax} = 6.78$, $g_{Ay} = 5.07$, and $g_{Az} = 1.95$ (see arrows in Fig. 6, inset), very similar, but not identical, to the change induced by a shift to pH 8.0. Interestingly, the same ferric EPR spectrum was observed at pH 6.5 and 8.0 with catechol (or pyrogallol) bound to the heme distal side. The loss of the pH dependence of the ferric EPR spectrum of BPC upon binding of the substrates is consistent with the phenolic oxygens having displaced the structural water molecules and/or making more tight H-bonds to His57 and Asn130, in total agreement with the crystal structures [Figs. 1(B) and [3]]. Moreover, the changes on the ferric spectrum of BPC were observed at both pH 6.5 and pH 8.0, thus indicating that the access and binding of catechol and pyrogallol at the heme distal side occurs at all pH values. In contrast, the total absence of spectral changes in the presence of guaicol confirms that it does not bind in proximity to the heme iron, as found in the crystal structures (Fig. 3). Interestingly, incubation of BLC with all three substrates showed no changes in the ferric EPR spectrum, indicating that either the access to

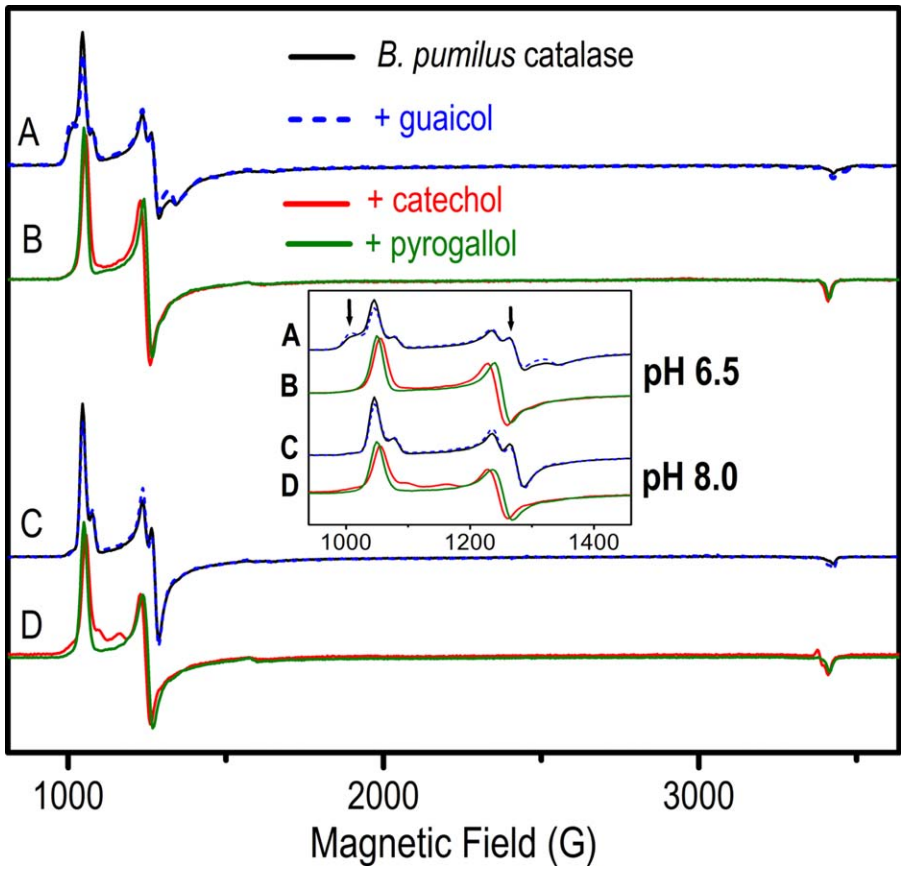

Figure 6

The 9-GHz EPR spectra of ferric BPC catalase with bound catechol, pyrogallol, and guaiacol. The enzyme was incubated with a high excess of each substrate (see description in Experimental section) and both the enzyme and substrate were initially at pH 6.5 (A and B) or 8.0 (C and D). The Inset shows an expansion of the lower field region of the spectrum (the $g \approx 6$ region). Experimental conditions: spectra were recorded at 4 K, 1 mW microwave power, 4 G modulation amplitude, 100 kHz modulation frequency.

the heme distal side, or the binding configuration, is not favorable in BLC.

DISCUSSION

The search for an unusual small subunit catalase-peroxidase with a penicillin oxidase activity in BPC B6033[2] began with the determination of the strain's genomic sequence,[11] which revealed a single heme catalase gene and two manganese catalase genes, but no catalase-peroxidase or peroxidase-like genes. We therefore focused our attention on the single heme-containing catalase, which proved to be kinetically and structurally similar to most other small subunit heme-containing catalases, but with an associated broad-spectrum peroxidase activity. This perhaps explains why it was previously mistaken for a catalase-peroxidase.[2]

A multiplicity of mechanisms by which peroxidases oxidize substrates have evolved, but the most common involves substrate binding on the heme distal side at the so-called δ-heme edge,[41] where their efficient oxidation involves the Fe^{IV}=O $Por^{\bullet+}$ intermediate. An alternative mechanism is found in cytochrome c peroxidase where guaiacol and phenol bind at two sites close to the surface, despite the δ-heme edge location being available, and are oxidized via the [Fe^{IV}=O $Tyr_{71}^{\bullet+}$] intermediate.[42] Lactoperoxidase is even more versatile with aromatic substrates and inorganic ions binding at multiple sites at the δ-heme edge, along the access channel to the heme site and at the enzyme surface,[43] and their oxidation being mediated by the Fe^{IV}=O $Por^{\bullet+}$ intermediate, or via a Tyr-based radical intermediate in the case of the more bulky ABTS.[44]

The observed peroxidase reactivity of BPC with polyphenols as substrates suggested the existence of substrate binding sites and this was confirmed in the identification of three binding sites in the crystal structures of six different ligand-protein complexes. The site closest to the heme accommodated only pyrogallol and catechol

suggesting a stereochemical requirement for the ortho relationship of two of the hydroxyl groups. This binding site was a surprise because it had long been thought that, unlike peroxidases, the narrow access channel to the heme active site of catalases would restrict access to only small oxidants and ligands such as H_2O_2, cyanide and some alcohols, and confer high efficiency for the disproportionation of hydrogen peroxide (catalase reaction). However, aminotriazole is not that much smaller than the polyphenols and it reacts with the imidazole of the essential distal side histidine, as observed in crystals of human erythrocyte catalase[34] and *Penicillium vitale* catalase.[45] The second binding site of BPC catalase is at the junction of the broad conical opening and the narrow, hydrophobic portion of the channel extending 12 Å to the heme. Comparison of this channel-binding site with similar regions in other catalases reveals potential conflicts in all cases that would interfere with binding, an indication that binding of polyphenols at this site may not be universal among catalases. This would be consistent with BPC, as a soil organism, frequently encountering polyphenols in its environment and adapting to their use in one or more aspects of cellular metabolism. One can envision the antioxidant effectiveness of the catalase being enhanced by a greater peroxidatic activity using polyphenols at low H_2O_2 concentrations, or that metabolism of polyphenols by catalase provides additional carbon sources for cellular metabolism. The range of catalases that bind and use polyphenols is currently being investigated.

The existence of multiple binding sites for peroxidatic substrates in an enzyme that is predominantly a catalase, both from structural and kinetics characteristics is significant for several reasons. The binding site in the heme cavity clearly demonstrates accessibility to a catalytically important part of the protein that was thought to be inaccessible in catalases. In fact, this binding site would not be accessible in Compound I because the ferryl-oxo oxygen would stereochemically prevent access to the heme iron and distal His and Asn required for binding. However, the very fact that access is possible suggests that direct donation of an electron (and a proton) to the Fe^{IV}=O $Por^{\bullet+}$ is possible. This differs from a typical peroxidase-substrate,[41] but the outcome is the same, Compound II or Fe^{IV}-OH Por. The second substrate-binding site in the main channel associated with Asp110 is 12 Å from the heme iron, making possible the direct electron transfer for reduction of the ferryl-oxo species at biologically relevant rates. In addition, this site is 3-4 Å from Tyr164, which with Trp165 (bridged by Asp 447) could act as potential relays in the electron transfer pathway to the heme similar to the situation in certain peroxidases.[42–44] The third binding site near Cys461 would require a longer electron transfer pathway, possibly involving Tyr464 and Tyr485 to Trp165 if it is a functional site.

The peroxidase activity of BPC, like the oxidase activity of BLC, begs the question of whether or not the "monofunctional" nomenclature associated with heme catalases is accurate and should be used. While preciseness dictates that it should not be used, it is also clear that the names catalase-peroxidase and catalase-oxidase are also inappropriate. The former name is already associated with a distinct family of enzymes, but more importantly, not all catalases have an oxidase activity (BLC does but BPC does not) and not all catalases have a peroxidase activity (BPC does but *E. coli* KatE does not[12]). It is also relevant that where the oxidase or peroxidase activities have been confirmed as exceeding the high background rates of substrate autooxidation, the turnover rates are very low (10–20 s^{-1}) in comparison to the more predominant catalase activity (usually $>$200,000 s^{-1}). Therefore, it is probably more accurate to refer to members of this family simply as "heme-containing or heme catalases," and then indicate on a case-by-case basis whether or not the enzyme possesses auxiliary activities.

Until recently, catalases and peroxidases were thought to differ in the mechanism of reduction of the common Fe^{IV}=O $Por^{\bullet+}$ intermediate with catalases using H_2O_2 in a two-electron reduction and peroxidases using a variety of substrates in two subsequent one-electron reductions. It has now become evident that there is more overlap than initially realized between the two families. For example, while most peroxidases do not show substantial catalase-like reactivity, catalase-peroxidases do but only because they contain an unusual cross-linked structure of three side chains, Met-Tyr-Trp on the heme distal side. In addition, it is now clear that certain catalases can use organic substrates as electron donors to support a low-level peroxidatic reaction, something that was first reported over 60 years ago for BLC.[10] The protein structures differ significantly with catalases using two distal side catalytic residues, His and Asn, situated in a very small cavity accessed through a narrow channel surrounded in a shell of hydrophobic residues, whereas peroxidases have a much more accessible heme cavity. Furthermore, the catalatic reaction occurs entirely within the heme cavity in both catalases and catalase-peroxidases, whereas peroxidases are more variable in the strategy used for the reaction with substrates. In some peroxidases, the substrate can only bind close to the heme-edge while in others, including catalase-peroxidases, the substrates can also bind far from the heme and employ long-range intramolecular electron transfer and protein-based radical intermediates to reduce the high-valent heme intermediates.[42,44] The peroxidatic reaction in BPC appears to be unique among catalases in employing both strategies with the polyphenols binding remotely at two different sites and also able to access the heme. The multiplicity of substrate binding sites in relatively close proximity to the heme also

suggests the intriguing possibility of a mechanism whereby substrate binding facilitates the peroxidase reaction by slowing the predominant catalase reaction.

REFERENCES

1. Nicholls P, Fita I, Loewen PC. Enzymology and structure of catalases. Adv Inorg Chem 2001;51:51–106.
2. Sangar S, Pal M, Moon LS, Jolly RS. A catalase-peroxidase for oxidation of β-lactams of their (R)-sulfoxides. Bioresource Technol 2012;115:102–110.
3. Chelikani P, Fita I, Loewen PC. Diversity of structure and properties among catalases. Cell Mol Life Sci 2004;61:192–208.
4. Vetrano AM, Heck DE, Mriano TM, Mishin V, Laskin DL, Laskin JD. Characterization of the oxidase activity in mammalian catalase. J Biol Chem 2005;280:35372–35381.
5. Ogel ZB, Yuzugullu Y, Mete S, Bakir U, Kpton Y, Sutay D, Demir AS. Production, properties and application to biocatalysis of a novel extracellular alkaline phenol oxidase from the thermophilic fungus *Scytalidium thermophilum*. Appl Microbiol Biotechnol 2006;71:853–862.
6. Kocabas DS, Bakir U, Phillips SEV, McPherson MJ, Ogel ZB. Purification, characterization, and identification of a novel bifunctional catalase-phenol oxidase form *Scytalidium thermophilum*. Appl Microbiol Biotechnol 2008;79:407–415.
7. Yuzugullu Y, Trinh CH, Farnhurst L, Ogel ZB, McPherson MJ, Pearson AR. Investigating the active center of the *Scytalidium thermophilum* catalase. Acta Crystallograph 2013;F69:369–375.
8. Yuzugullu Y, Trinh CH, Smith MA, Pearson AR, Phillips SEV, Kocabas DS, Bakir U, Ogel ZB, McPherson MJ. Structure, recombinant expression and mutagenesis studies of the catalase with oxidase activity from *Scytalidium thermophilum*. Acta Crystallograph 2013; D69:398–408.
9. Singh R, Wiseman B, Deemagarn T, Donald LJ, Duckworth HW, Carpena X, Fita I, Loewen PC. Catalase-peroxidases (KatG) exhibit NADH oxidase activity. J Biol Chem 2004;279:43098–43106.
10. Tauber H. Oxidation of pyrogallol to purpurogallin by crystalline catalase. J Biol Chem 1953;205:395–400.
11. Villanueva J, Switala J, Ivancich A, Loewen PC. Genome sequence of *Bacillus pumilus* MTCC B6033. Genome Announc 2014;2:e00327-14.
12. Loewen PC, Switala J. Purification and characterization of catalase HPII from *Escherichia coli* K12. Biochem Cell Biol 1985;64:638–646.
13. Switala J, Loewen PC. Diversity of properties among catalases. Arch Biochem Biophys 2002;401:145–154.
14. Rørth M, Jensen PK. Determination of catalase activity by means of the Clark oxygen electrode. Biochim Biophys Acta 1967;139:171–173.
15. Childs RE, Bardsley WG. The steady-state kinetics of peroxidase with 2,2'-azino-di-(3-ethylbenzthiazoline-6-sulphonic acid) as chromogen. Biochem J 1975;145:93–103.
16. Regelsberger G, Jakopitsch C, Engleder M, Rüker F, Peschek G, Obinger C. Spectral and kinetic studies of the oxidation of monosubstituted phenols and anilines by recombinant *Synechocystis* catalase-peroxidase compound I. Biochemistry 1999;38:10480–10488.
17. Mulvey MR, Sorby PA, Triggs-Raine BL, Loewen PC. Cloning and physical characterization of *katE* and *katF* required for catalase HPII expression in *Escherichia coli*. Gene 1988;73:337–345.
18. Sudhamsu J, Kabir M, Airola MV, Patel BA, Yeh SR, Rousseau DL, Crane BR. Co-expression of ferrochelatase allows for complete heme incorporation into recombinant proteins produced in *E. coli*. Prot Exp Purif 2010;73:78–82.
19. Kabsch W. XDS. Acta Crystallograph 2010;D66:125–132.
20. Leslie AGW, Powell HR. Processing diffraction data with MOSFLM. Evol Methods Macromol Crystallogr 2007;245:41–51
21. Winn MD, Ballard CC, Cowtan KD, Dodson EJ, Emsley P, Evans PR, Keegan RM, Krissinel EB, Leslie AGW, McCoy A, McNicholas SJ, Murshudov GN, Pannu NS, Potterton EA, Powell HR, Read RJ, Vagin A, Wilson KS. Overview of the CCP4 suite and current developments. Acta Crystallograph 2011;D67:235–242.
22. Vagin A, Teplyakov A. MOLREP: an automated program for molecular replacement. J Appl Cryst 1997;30:1022–1025.
23. Loewen PC, Carpena X, Rovira C, Ivancich A, Perez-Luque R, Haas R, Odenbreit S, Nicholls P, Fita I. Structure of *Helicobacter pylori* catalase, with and without formic acid bound, at 1.6 Å resolution. Biochemistry 2004;43:3089–3103.
24. Murshudov GN, Vagin AA, Dodson EJ. Refinement of macromolecular structures by the maximum-likelihood method. Acta Crystallograph 1997;D53:240–255.
25. Emsley P, Lohkamp B, Scott WG, Cowtan K. Features and development of Coot. Acta Crystallograph 2009;D66:486–501.
26. Ho BK, Gruswitz F. HOLLOW: generating accurate representations of channel and interior surfaces in molecular structures. BMC Struct Biol 2008;8:49–54.
27. Ivancich A, Jouve HM, Sartor B, Gaillard J. EPR investigation of Compound I in *Proteus mirabilis* and bovine liver catalases: formation of porphyrin and tyrosyl radical intermediates. Biochemistry 1997;36:9356–9364.
28. Tirumalai MR, Rastogi R, Zamani N, O'Bryant WE, Allen S, Diouf F, Kwende S, Weinstock GM, Venkateswaran KJ, Fox GE. Candidate genes that may be responsible for the unusual resistances exhibited by *Bacillus pumilus* SAFR-032 spores. PLoS One 2013;8:e66012.
29. Singh R, Wiseman B, Deemagarn T, Jha V, Switala J, Loewen PC. Comparative study of catalase-peroxidases. Arch Biochem Biophys 2008;471:207–214.
30. Wiseman B, Carpena, X, Feliz M, Donald LJ, Pons M, Fita I, Loewen PC. Isonicotionic acid hydrazide conversion to isonicotinyl-NAD by catalase-peroxidases. J Biol Chem 2010;285:26662–26673.
31. Colin J, Jakopitsch C, Obinger C, Ivancich A. The reaction of *Synechocystis* catalase-peroxidase (KatG) with isoniazid investigated by multifrequency (9-285 GHz) EPR spectroscopy. Appl Magn Reson 2010;37:267–277.
32. Singh R, Switala J, Loewen PC, Ivancich A. Two [Fe(IV)=O Trp•] intermediates in *M. tuberculosis* catalase-peroxidase discriminated by multifrequency (9-285 GHz) EPR spectroscopy: reactivity toward isoniazid. J Am Chem Soc 2007;129:15954–15963.
33. Colin J, Wiseman B, Switala J, Loewen PC, Ivancich A. Distinct role of specific tryptophans in facilitating electron transfer or as [Fe(IV)=O Trp•] intermediates in the peroxidase reaction of *Burkholderia pseudomallei* catalase-peroxidase: a multifrequency EPR spectroscopy investigation. J Am Chem Soc 2009;131:8557–8563.
34. Putnam CD, Arvai AS, Bourne Y, Tainer JA. Active and inhibited human catalase structures: ligand and NADPH binding and catalytic mechanism. J Mol Biol 2000;296:295–309.
35. Carpena X, Soriano M, Klotz M, Duckworth HW, Donald LJ, Melik-Adamyan W, Fita I, Loewen PC. Structure of the clade 1 catalase, CatF of *Pseudomonas syringae*, at 1.8 Å resolution. Proteins 2003;50:423–436.
36. Jha V, Louis S, Chelilani P, Carpena X, Donald LJ, Fita I, Loewen PC. Modulation of heme orientation and binding by a single residue in catalase HPII of *Escherichia coli*. Biocehmistry 2011;50:2101–2110.
37. Díaz A, Loewen PC, Fita I, Carpena X. Thirty years of heme catalases structural biology. Arch Biochem Biophys 2012;525:102–110.
38. Benecky MJ, Frew JE, Scowen N, Jones P, Hoffman BM. EPR and ENDOR detection of compound I from *Micrococcus lysodeikticus* catalase. Biochemistry 1993;32:11929–11933.
39. Jakopitsch C, Obinger C, Un S, Ivancich A. Identification of Trp106 as the tryptophanyl radical intermediate in *Synechocystis* PCC6803 catalase-peroxidase by multifrequency Electron Paramagnetic Resonance spectroscopy. J Inorg Biochem 2006;100:1091–1099.
40. Carpena X, Wiseman B, Deemagarn T, Herguedas B, Ivancich A, Singh R, Loewen PC, Fita I. Roles of Arg426 and Trp111 in the modulation of NADH oxidase activity of the catalase-peroxidase KatG from *Burkholderia pseudomallei* inferred from pH-induced structural changes. Biochemistry 2006;45:5171–5179.

41. Gumiero A, Murphy EWJ, Metcalfe CL, Moody PCE, Raven EL. An analysis of substrate binding interactions in the heme peroxidase enzymes: a structural perspective. Arch Biochem Biophys 2010;500: 13–20.
42. Miner KD, Pfister TD, Hosseinzadeh P, Karaduman N, Donald LJ, Loewen PC, Lu Y, Ivancich A. Identifying the elusive sites of tyrosyl radicals in cytochrome c peroxidase: implications for oxidation of substrates bound at a site remote from the heme. Biochemistry 2014;53:3781–3789.
43. Sharma S, Singh AK, Kaushik S, Sinha M, Singh RP, Sharma P, Sirohi H, Kaur P, Singh TP. Lactoperoxidase: structural insights into the function, ligand binding and inhibition. Int J Biochem Mol Biol 2013;4:108–128.
44. Fielding AJ, Singh R, Boscolo B, Loewen PC, Ghibaudi EM, Ivancich A. Intramolecular electron transfer versus substrate oxidation in lactoperoxidase: investigation of radical intermediates by stopped-flow absorption spectrophotometry and (9-285 GHz) Electron Paramagnetic Resonance spectroscopy. Biochemistry 2008;47: 9781–9792.
45. Borovik AA, Grebenko AI, Melik-Adamyan WR. X-ray diffraction study of *Penicillium vitale* catalase in complex with aminotriazole. Cryst Rep 2011;56:590–595.